MODELLING THERMAL EFFECTS IN YOUNG CONCRETE
Cracking in reinforced concrete caused by temperature rise generated by hydration

Agnes Nagy, M.Sc.,Research Assistant
Division of Structural Engineering
Lund Institute of Technology , Sweden

Sven Thelandersson, Dr., Professor
Division of Structural Engineering
Lund Institute of Technology , Sweden

Abstract

This report is concerned with cracking in reinforced concrete caused primarily by temperature rise generated by hydration of the cement. The cracking is caused by tensile stresses in the concrete due to restraint of thermal contraction.

Based on given temperature history and a very simple constitutive model for young concrete theoretical simulations of the thermal stresses were made. This was accomplished using a finite element computer program. The results of the theoretical model were validated against test results and a parametric investigation was made. The model also made it possible to investigate the effect of reinforcement in concrete on the early thermal stresses.

The theoretical model shows a good conformity with test results indicating that an accurate prediction of early age thermal stresses can be made in a simple way if the stiffness development of the young concrete is known from laboratory tests. The presence of reinforcement does not improve the ability to avoid cracking due to thermal stresses.

Keywords

thermal cracking; reinforced concrete; restraint; stiffness;

1. Introduction

One of the major causes of cracking in structures is internal stresses due to cooling of the concrete from the increased temperature level generated by hydration of the cement.

Early thermal cracking mainly occurs when the thermal movement is prevented by external restraint e.g. if a wall is cast against an old set concrete. As the wall cools it is restrained by the

adjacent pours and cracking may develop if the restraint stresses produced by the cooling process exceed the tensile strength of the concrete. Thermal cracking can also be caused by temperature gradients within members and by temperature variations in the environment.

The phenomenon of thermally induced cracking has come into focus during the last 10-15 years when experience showed that thermal effects contributed to cracking not only in mass concrete but also in medium-thick structures. Contributions by Springenschmid /1/ and Breitenbücher /2/ can be mentioned here regarding experimentally obtained thermal stresses. Their results indicate the dependence of cracking not only on temperature history and rate of cooling but on the mechanical behaviour of the concrete at early ages as well.

An important contribution to this field has been given by Emborg /3/. His principal idea was to measure early age thermal stresses in laboratory tests and evaluate the risk for cracking with emphasis on the time-dependent material characteristics of the young concrete. Emborg developed and verified a rather advanced constitutive model to predict early age thermal stresses.

The purpose of the present paper is to see if thermal stresses in young concrete can be predicted by a simplified model with few material parameters. The advantage of such a model is that it can easily be used for practical purposes. The verification of the model is based on the comprehensive test data presented by Emborg /3/. The role of reinforcement in the early age concrete prior to cracking is also investigated. A parametric study is performed in order to identify which mechanical properties are most important for the development of thermal stresses.

2. Mechanical model

The theoretical model has been formulated assuming uniaxial stress and restraint conditions. Concrete and reinforcement are modelled separately and the interaction between concrete and steel is simulated by means of shear forces acting at the interface between the two materials. A similar type of model was used by Hagman /4/.

The incremental stress-strain relation for the steel is given by

$$\Delta\sigma_s = E_s \left[\Delta\varepsilon_s - \alpha_s * \Delta T \right] \qquad (1)$$

where $\Delta\sigma_s$ and $\Delta\varepsilon_s$ are stress and strain increments of the steel, ΔT is the temperature increment at time t, α_s is the coefficient of thermal dilatation of the steel and E_s is the elastic modulus of steel. Both α_s and E_s are assumed to be independent of temperature.

The corresponding relation for concrete (index c) is

$$\Delta\sigma_c = E_c(t) \left[\Delta\varepsilon_c - \alpha_c * \Delta T \right] \qquad (2)$$

The elastic modulus E_c for concrete is assumed to be age-dependent. The coefficient of thermal dilatation was assumed to be independent of age but with different values α_{ce} and α_{cc} during expansion

($\Delta T>0$) and contraction ($\Delta T<0$), respectively.

Aging was described by the well-known concept of equivalent maturity time t_e, defined by

$$t_e = \int_0^t \beta_t \, dt \tag{3}$$

where β_t is a maturity function described by the Arrhenius expression

$$\beta_t = \exp \frac{U_h}{R} \left(\frac{1}{293} - \frac{1}{T} \right) \tag{4}$$

Here T is concrete temperature, U_h is activation energy of hydration and R is the universal gas constant. The maturity function takes into account the changed reaction rate of hydration at temperatures different from 20°C.

Equations (2) and (3) give a very simple description of the mechanical response of the young concrete. The parameter E_c is taken from creep tests performed by Emborg /3/. The tests were carried out on young concrete loaded at different early ages. The total time-dependent deformation $\varepsilon(t_e,t_e')$ at time t_e from a loading at time $t_e' \leq t_e$, is defined as:

$$\varepsilon \left(t_e, t_e'\right) = J \left(t_e, t_e'\right) \sigma \left(t_e'\right) \tag{5}$$

where $J(t_e,t_e')$ is the compliance function and $\sigma(t_e')$ is the stress applied at time t_e'. The compliance function is chosen to $1/E(t_e')$ i.e. to the inverse of the modulus of elasticity at time t_e'. This means that only an elastic part of the time-dependent deformation is taken into account neglecting creep deformations.

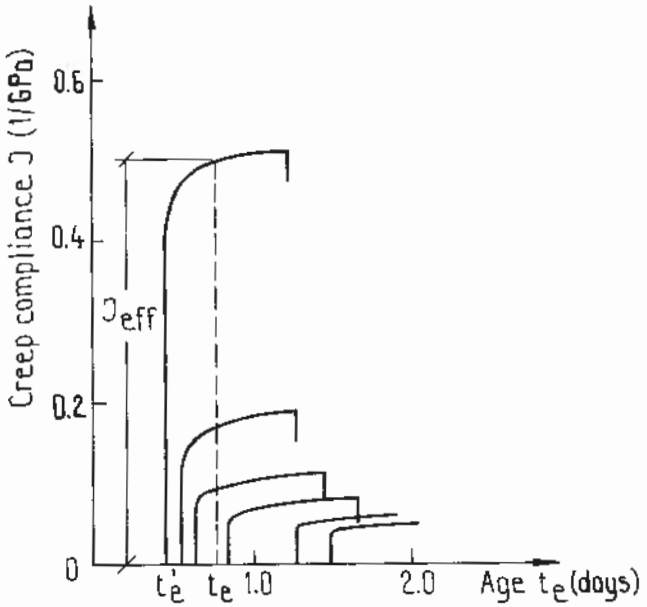

Fig.1. Creep in young concrete with the stress σ applied at different ages. An effective material stiffness E_{eff} is estimated from $E_{eff}=1/J_{eff}$.

In evaluating tests of the type shown in Fig.1, a certain amount of creep is included implicitly by using an elastic modulus $E_{eff}=1/J_{eff}$ where $J_{eff}=J(t_e'+5h,t_e')$. See Fig.1. The choice of reference time to 5 hours is arbitrary, but it is evident from Fig.1 that the result is not sensitive to this choice. The variation of E_{eff} with equivalent maturity time at loading is shown in Fig.5 for two types of concrete.

It should be pointed out that the stress-strain relation for very young concrete is non-elastic also for low stresses /5/. Some part of the strain is plastic in the sense that it is irreversible if the load is removed instantly (see Fig.2). This behaviour is most significant at very early age. With increasing age the behaviour becomes more elastic. At the time when actual unloading takes place in practical structures the approximation of elastic behaviour is reasonable.

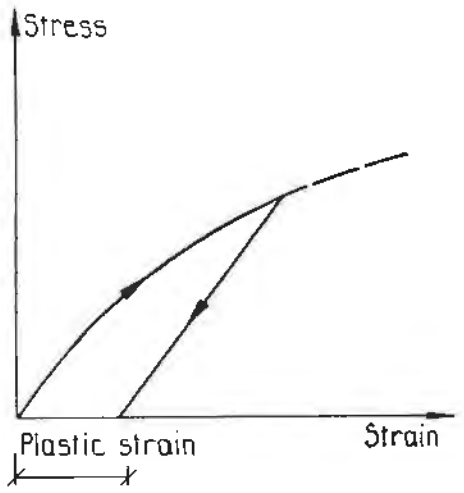

Fig.2. Typical stress-strain relation for very young concrete.

The behaviour of the interface between steel and concrete is described by the incremental relation

$$\Delta S = k(t)\left[\Delta u_c - \Delta u_s\right] \qquad (6)$$

where ΔS is the bond force increment (N/m) at the interface, Δu_c and Δu_s are incremental displacements in concrete and steel respectively and $k(t)$ is the bond stiffness, which may depend on age.

The constitutive relations (1),(2) and (5) in combination with standard kinematical and equilibrium relations describe the combined uniaxial behaviour of a reinforced concrete prism. See Fig.3. These relations were transformed into finite element (FEM) relations according to standard procedures /7/ and programmed as additional subroutines to a FEM program called CAMFEM /6/. The use of a step-by-step analysis with suitably chosen time steps gave the possibility of a rather accurate description of the uniaxial behaviour of the reinforced concrete.

This model was applied to a uniaxially reinforced concrete prism divided into 10 elements. Each finite element consists of three parts: concrete, steel and the interaction between these two modelled by a spring, see Fig.3.

3. Plain concrete

The model has been built up for reinforced concrete but simulation of plain concrete is possible by choosing a very small reinforcement area in relation to the concrete area and by setting the stiffness of the interface layer very small .

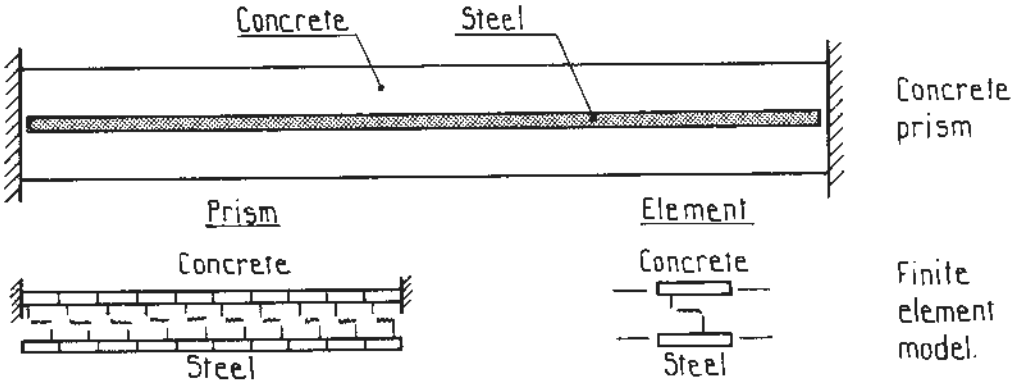

Fig.3. Modelling of reinforced concrete prism.

The results were validated against experimental data performed by Emborg /3/. The concrete quality and the restraint of the prism were prescribed in the same way as in the relaxation tests to achieve a good simulation of the test set-up and loading procedure. Two types of concrete (S279 and A300) are analysed. The axial movement at the ends of the prism was considered free from the start t=0, up to the time $t_{restraint}$. From this time onwards the prism was considered fully restrained, i.e. the axial displacements were fixed at both ends. The time $t_{restraint}$ coincides with the time when restraint was imposed in the tests /3/. In all the figures containing time axis, t=0 is defined as pouring time. Material characteristics are shown in Table 1.

The S279 and A300 types are relevant to concrete with normal and slow hardening rate, respectively. The cement used for the mix A300 also generates less heat during hydration. Different temperature histories were used for the two types of concrete as shown in Fig.4. These temperature variations correspond to cases when the concretes are used for a wall with thickness of 700 mm, see Emborg /3/. The material stiffness E_{eff} as a function of age is shown in Fig.5. The E_{eff}-curves in Fig.5 were evaluated from creep-tests, Emborg /3/,and are supposed to include plastic strain and partial creep of the young concrete.

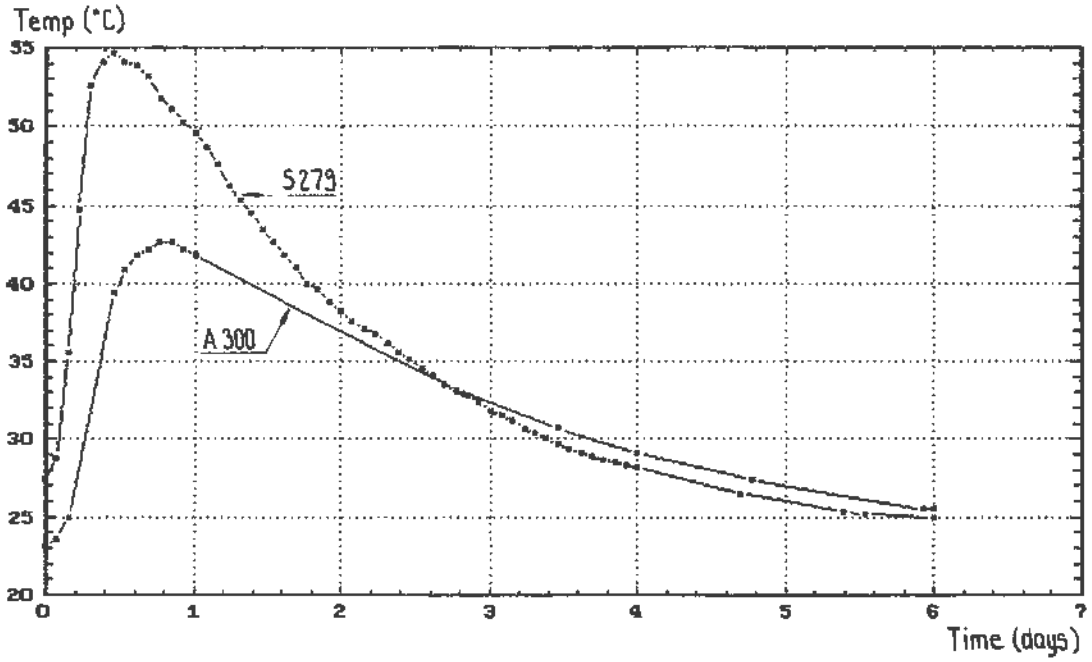

Fig.4. Temperature history for S279, A300 from Emborg /3/.

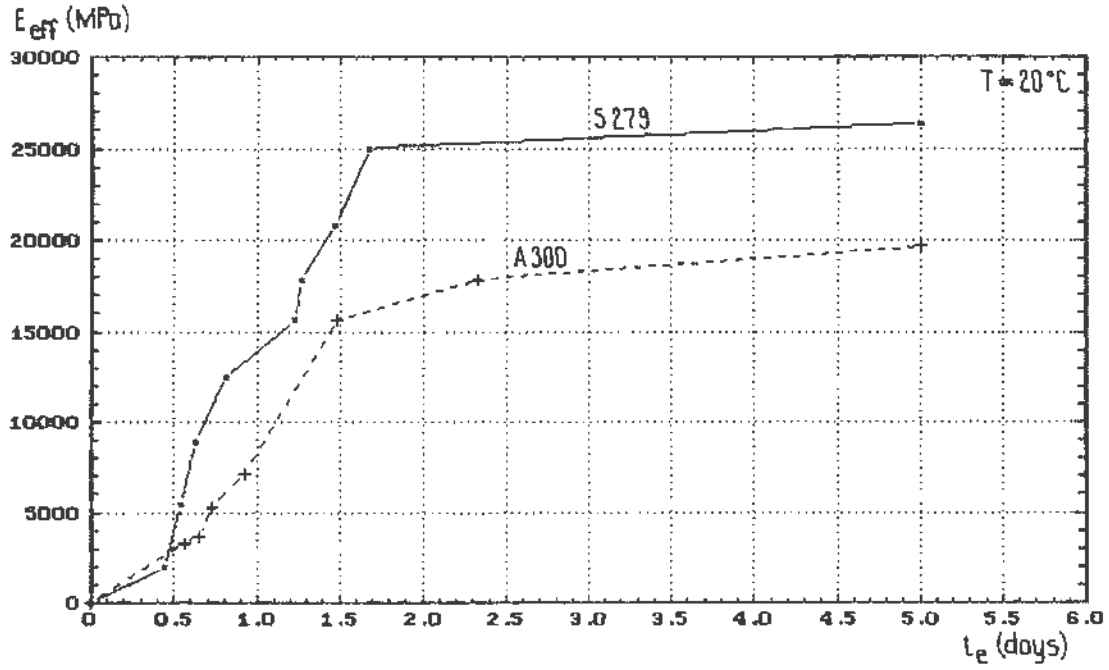

Fig.5. Effective stiffness E_{eff}, see Fig.1, evaluated from creep tests performed by Emborg /3/.

The results of the validation against tests are shown in Fig.6 and 7. It can be observed that the model gives a rather good conformity with the test results especially during the period with compressive stresses in the concrete. The tensile strength f_{ct} as a function of time taken from Emborg /3/ is also shown in Fig.6 and 7. In the tests, tension failure occurred in the specimens at stresses which were considerably lower than the strength. This could be explained by unintended eccentricity in the test set up.

To get an idea about sensitivity of the model a parametric investigation has been made :
-In Fig.8 the stress-development is compared for the two concrete types. The higher curing temperature in the case of S279 causes an earlier appearance of the maximum compressive stress, which is also slightly higher than for A300. The tensile strength for S279 is reached about two days after pouring whereas for A300 the stress at t=5.5 days is not even close to its tensile strength.

Table 1. Concrete characteristics

Concrete cement cont. [kg/m^3]	W/C	Thermal dilatation [10^{-6}/°C]		28 days E_c	f^{28}_{cc}	$t_{restraint}$
		α_{ce}	α_{cc}	[GPa]	[MPa]	[days]
S279	0.61	9.5	7.5	36.0	46.2	0.23
A300	0.54	11.5	7.5	35.2	56.7	0.35

S279 - Ordinary Portland Cement type I (Slite,Sweden)
A300 - Ordinary Portland Cement type II (Degerhamn,Sweden)

-In Fig.9 the normal S279 is shown with the restraint applied at the time $t_{restraint}$=0.23 days, which was necessary in the test since before this time the concrete was so plastic that no restraint could be applied. The same case (S279) was also simulated with $t_{restraint}$=0 days, as would be relevant for a structure in practice, for the sake of comparison.

An earlier restraint of the concrete gives a higher compressive stress in the beginning and a later appearance of the tensile stresses. This can be explained by the fact that early restraint includes the period when the greatest temperature changes take place and accordingly the restraint reactions become greater. With high compressive stress initially more time is needed for the structure to go through relaxation and reach the tensile strength. The difference between the two cases shown in Fig.9 is small, however, which means that the error in the test procedure is nonsignificant.

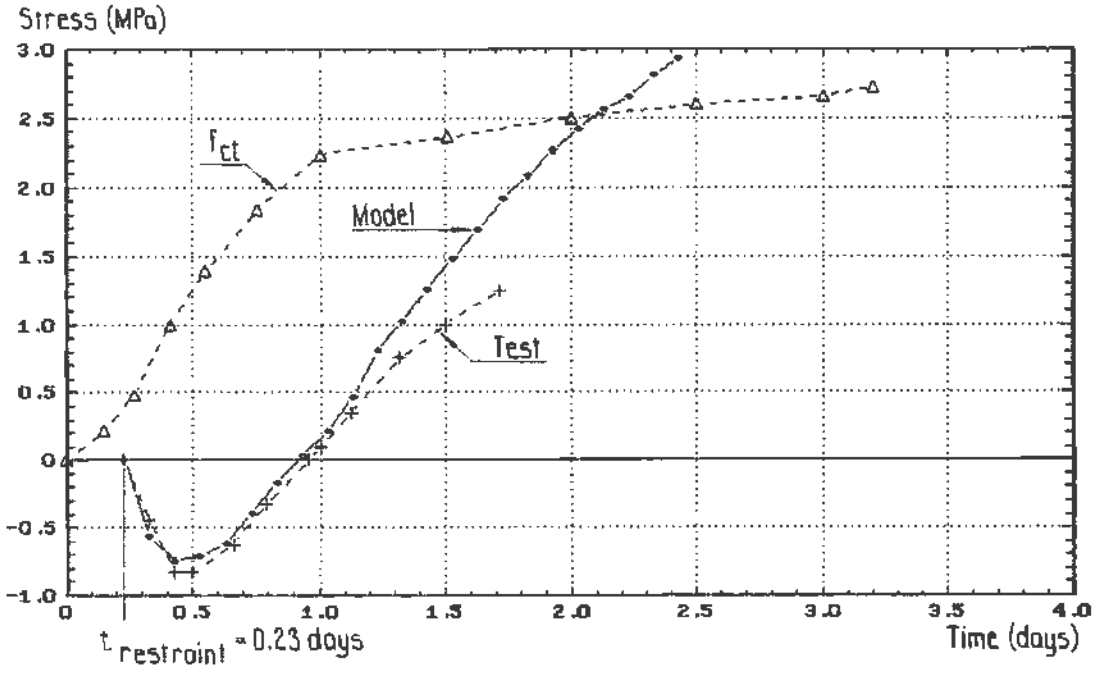

Fig.6. Stress development in concrete S279.

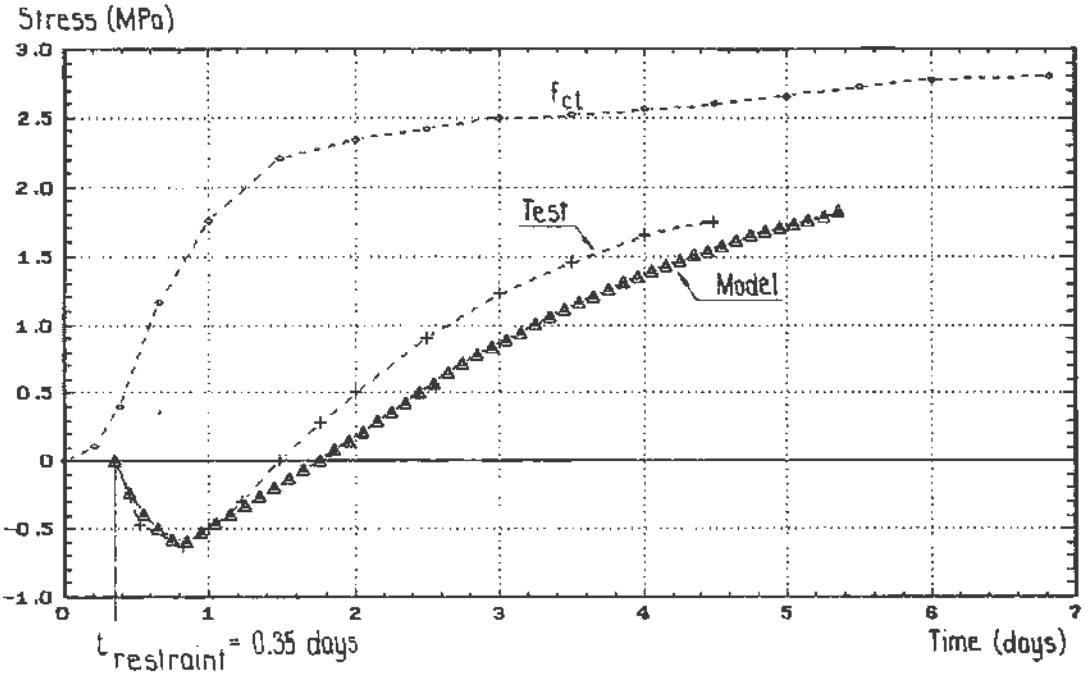

Fig.7. Stress development in concrete A300.

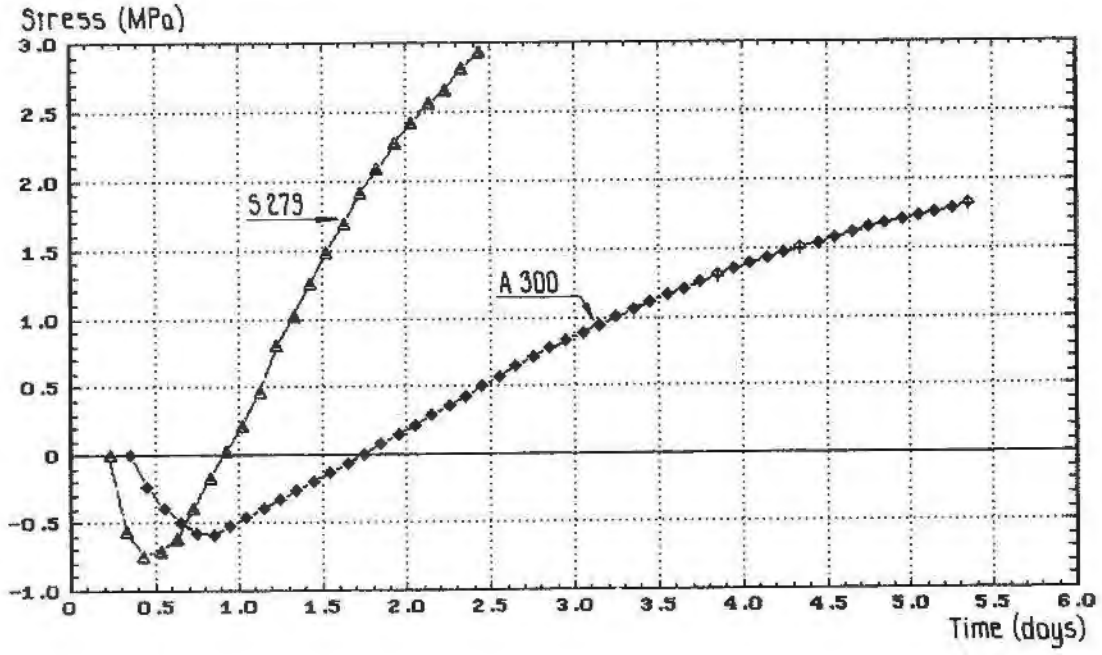

Fig.8. Comparison of stress development between S279 and A300.

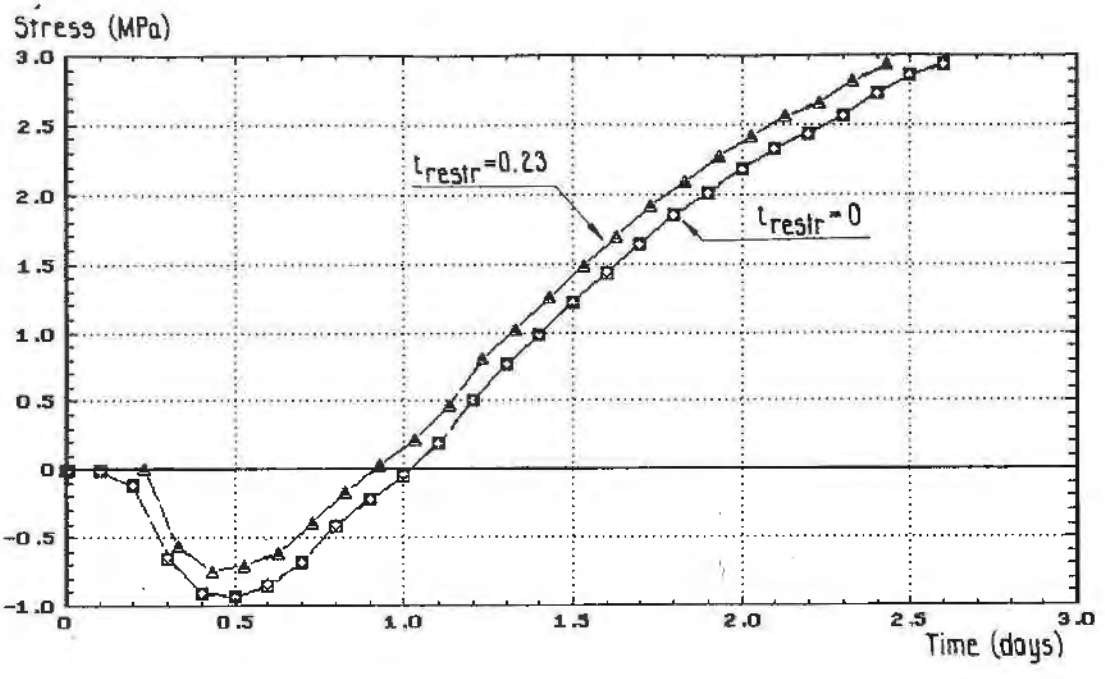

Fig.9. Influence of the time of application of restraint for S279.

-In Fig.11 the case S279 is compared with the same concrete but with increased curing temperature according to Fig.10. With increased temperature the maximum compressive stress is about the same as for normal S279, but the tensile stress increases much faster. One should expect that higher temperature causes higher compressive stresses, but a larger temperature increase during the initial stage does not create high stresses since the concrete stiffness has not been developed. Cooling from a higher level gives a more rapid increase in the tensile stresses, however.

-In Fig.13 the influence of a change in stiffness development according to Fig.12 is illustrated. An earlier development of E_c gives a significant increase in compressive stress, given that the temperature history is unchanged. This is an advantage since the tensile stresses during the cooling period become much smaller. This underlines the close relation between the E-modulus development and thermal stresses, i.e. the early age stiffness properties of the concrete are very important.

-In Fig.14 both the curing temperature and the E-modulus values are increased simultaneously. The maximum compressive stress becomes much higher but the tensile stress increases more rapidly than in the reference case. The positive influence of early stiffness development in the young concrete is obvious as well as the negative influence of increased temperature in reaching the tensile strength earlier. The model shows clearly the sensitivity of concrete to increased temperature at early ages.

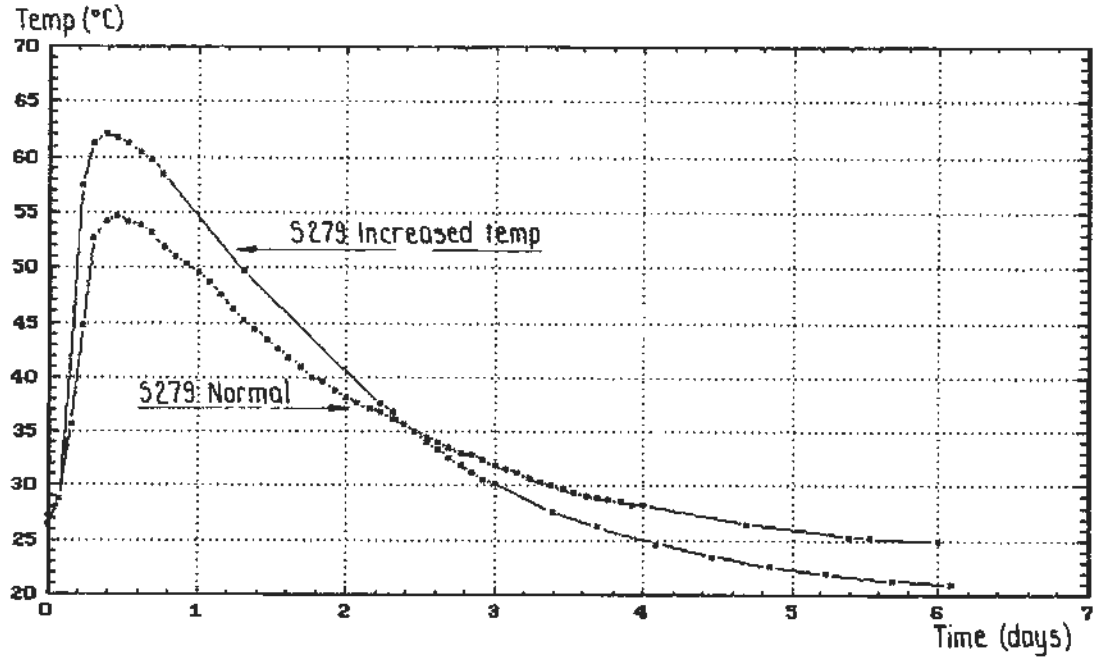

Fig.10. Increased temperature for S279.

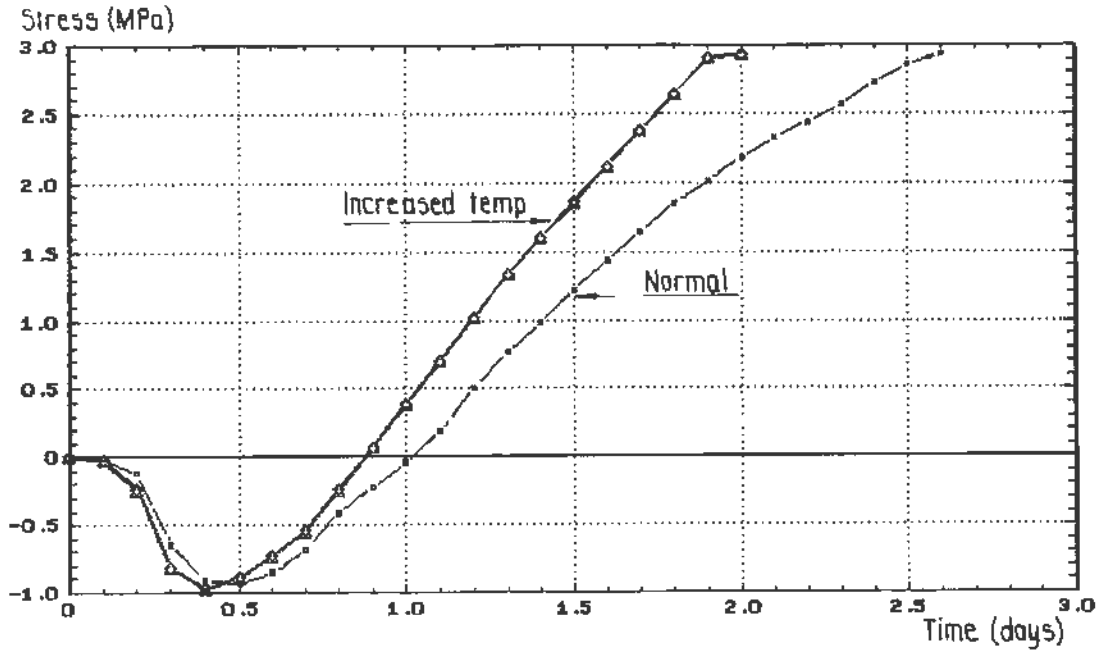

Fig.11. Simulation of increased temperature for S279.

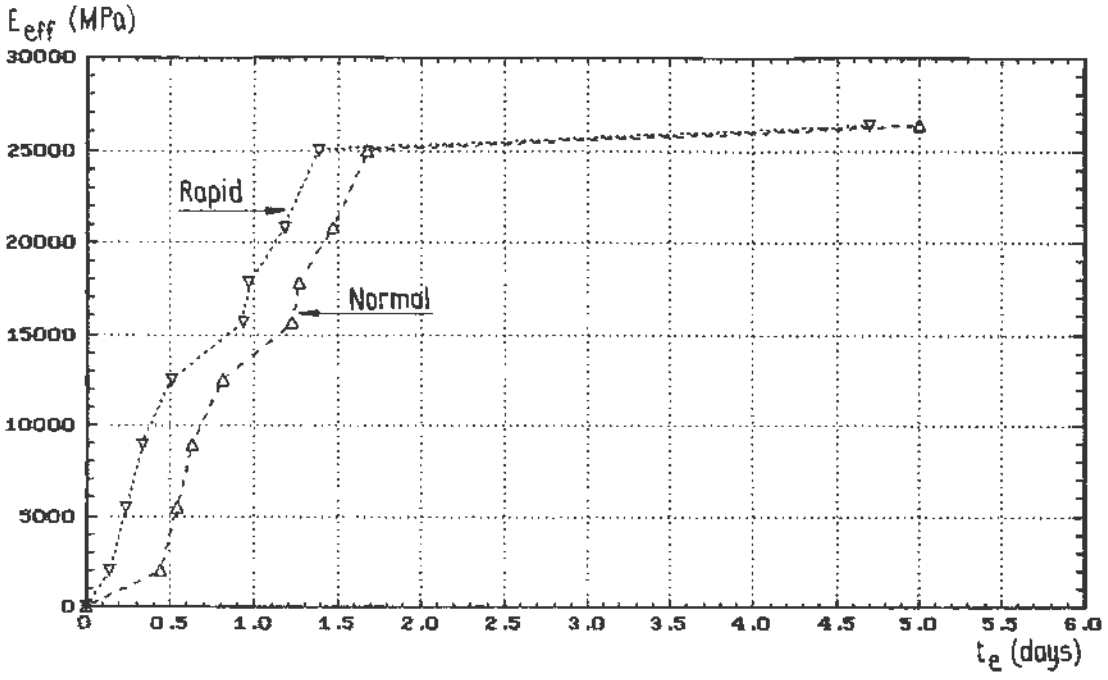

Fig.12. Rapid and normal development of stiffness for concrete S279.

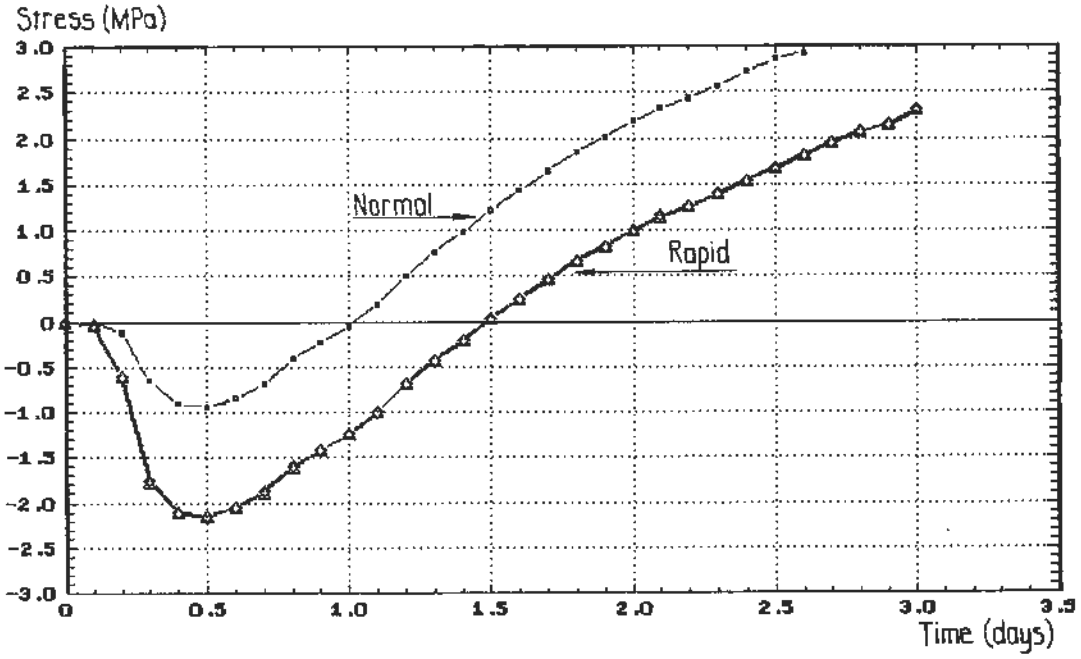

Fig.13. Influence of rapid development of material stiffness for S279.

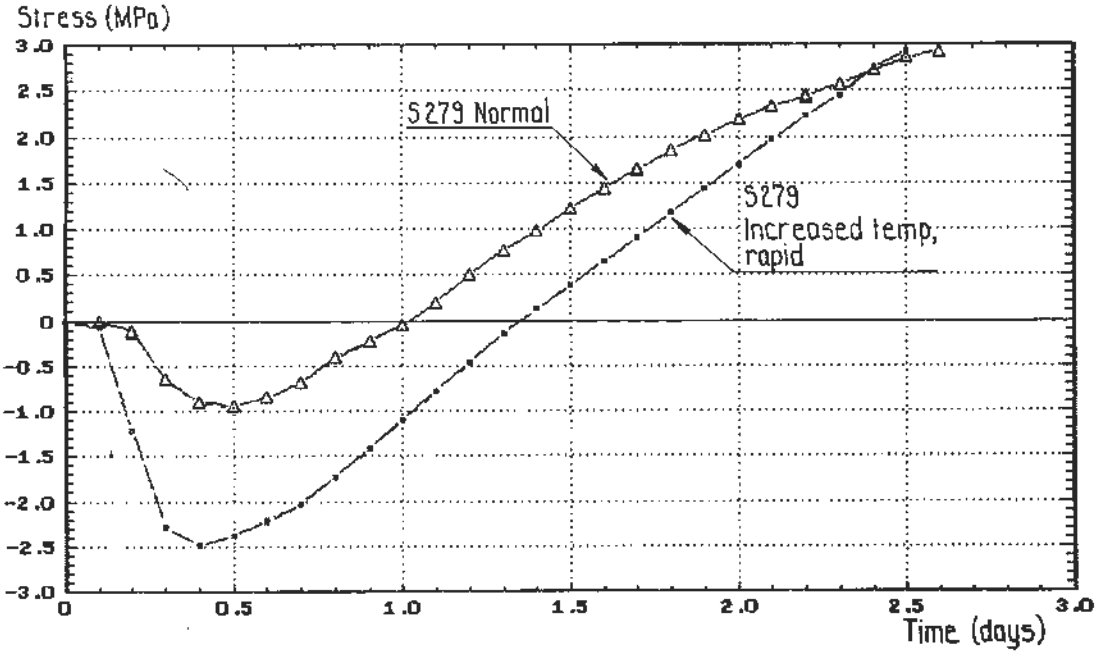

Fig.14. Simulation of increased temperature and rapid development of E_{eff} for S279.

4. Reinforced concrete

To simulate reinforced concrete, a certain percentage of reinforcement is placed in the concrete prism. The bond stiffness k(t) is assumed to have the same age dependence as the elastic modulus of the concrete. Thus, the following formula is valid :

$$k(t) = E(t) * \frac{k_{28}}{E_{28}} \qquad (7)$$

where E_{28} and k_{28} are the 28 days values of E_c and k . In the computations presented herein the ratio k_{28}/E_{28} was chosen to 0.022. The amount of reinforcement was 0.75 % .

The computed stress development in the concrete is shown in Fig.15 for S279 and Fig.16 for A300. In both cases the concrete was fully restrained and the steel was free to move. Practically there is no difference between concrete stresses in plain concrete and reinforced concrete for neither of the concrete types.
Thus, the model cannot point out any significant effects of the reinforcement in the early-age concrete prior to cracking.

In Fig.17 and 18 the stress in the reinforcement and the bond stress are shown for A300. A rather big difference can be observed between stresses in elements placed at the end of the prism and in the mid section. Both bond stress and steel stress are rather small.

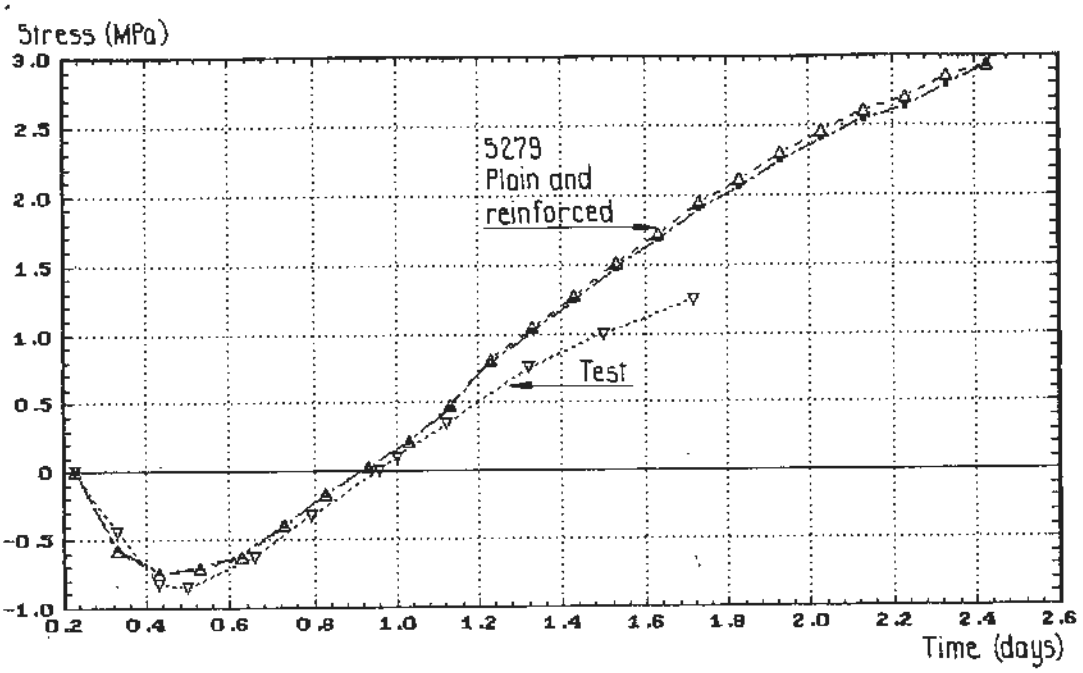

Fig.15. Effect of reinforcement on S279.

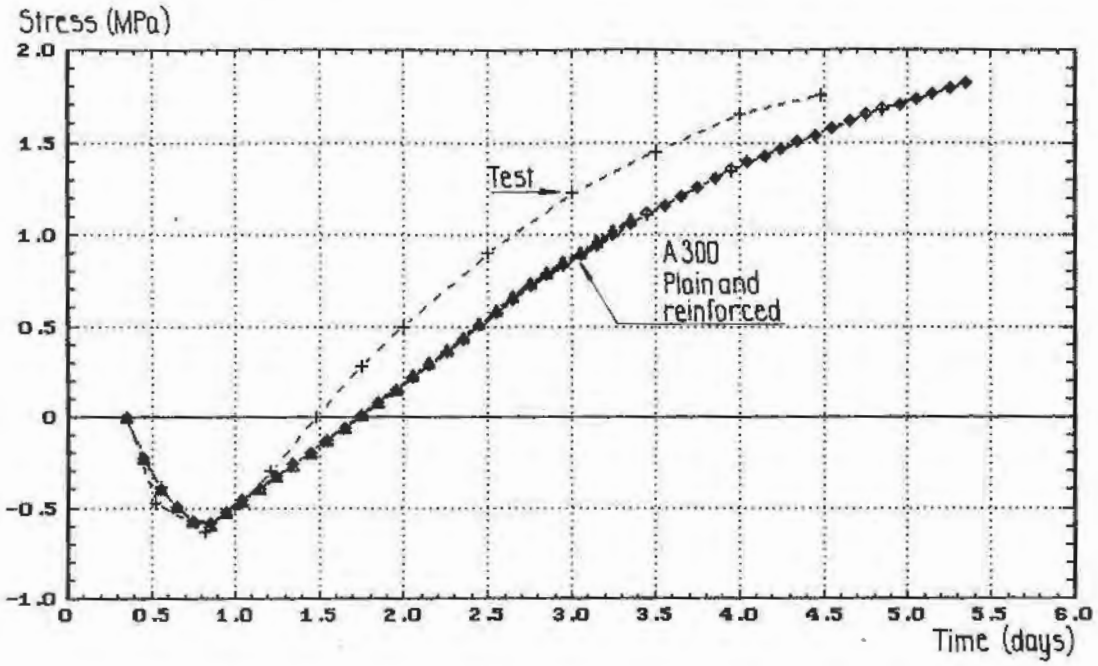

Fig.16. Effect of reinforcement on A300.

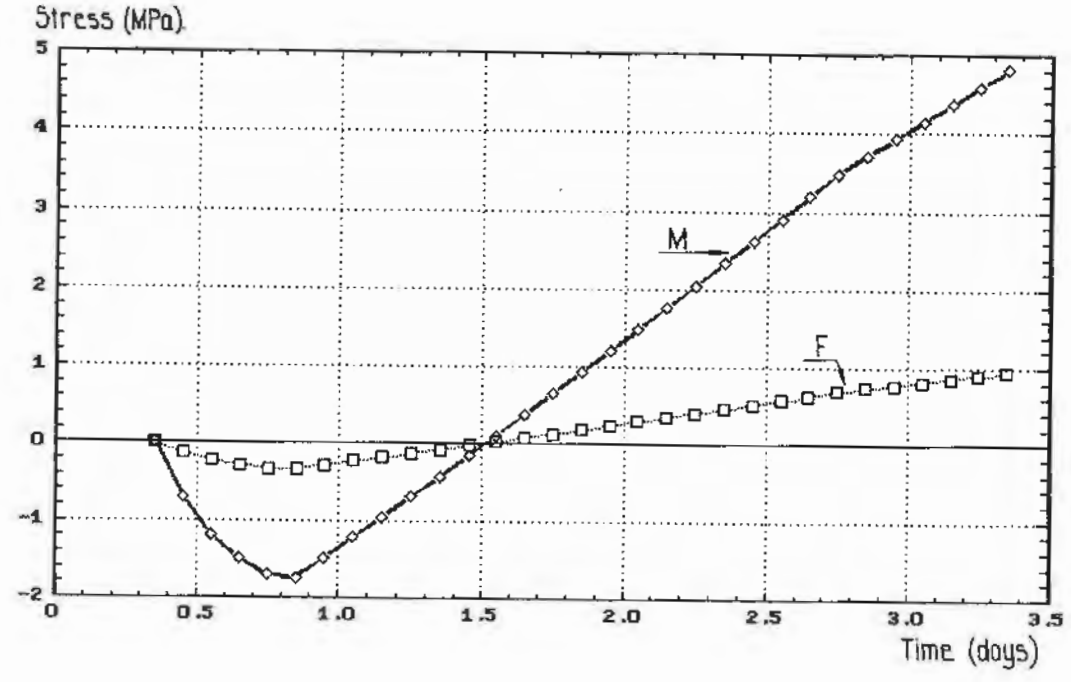

Fig.17. Stress in reinforcement in A300.
F-first element in the prism
M-mid section in the prism

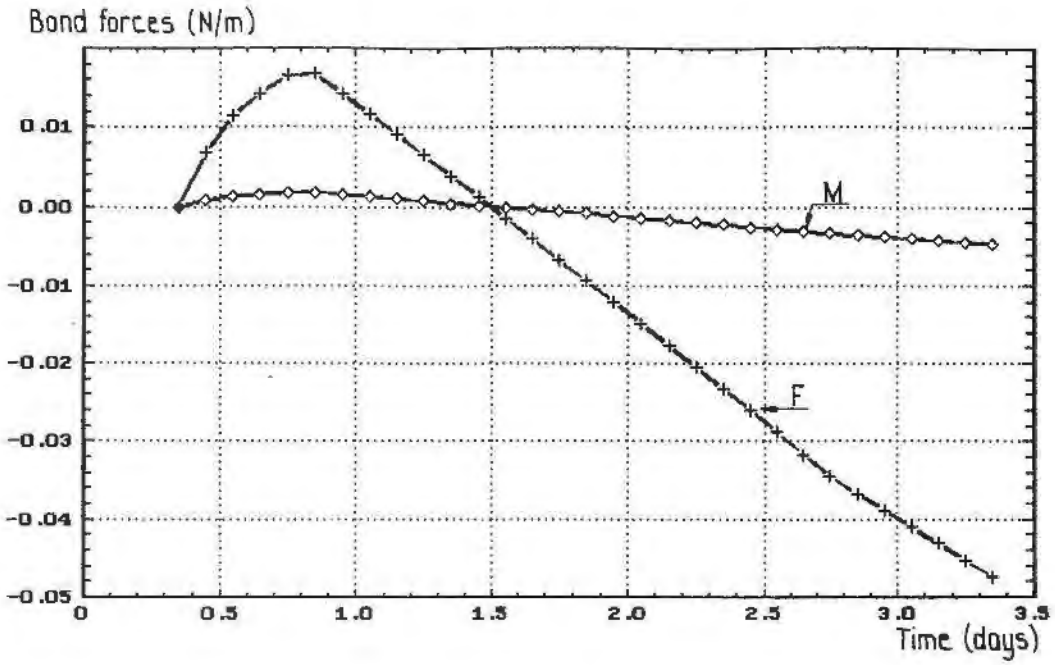

Fig.18. Bond stresses in A300.
F-first element in the prism
M-mid section in the prism

This is due to the fact that the reinforcement was not subjected to end restraint. To investigate the influence of boundary conditions, computations were made for two cases. In the first case the concrete was fully restrained and the steel was free at the ends. In the second case both concrete and steel were fully restrained at the ends.

In Fig.19 a comparison of the stresses in restrained concrete is made regarding free and restrained steel. As earlier observed the free steel did not improve the behaviour of the young concrete prior to thermal cracking. The same behaviour is valid when the steel is restrained and the two concrete stress curves are coincident. The stress in the reinforcement for the two cases is shown in Fig.20 . The restrained steel shows a significant increase in compressive stress in all elements independent of their position in the prism.

5. Summary and conclusions

Early thermal stresses in concrete were investigated by means of a very simple linear constitutive model. All computations have been made with a FEM program which made possible a parametric investigation of two types of concrete with normal hardening rate and with slow hardening rate. The computed stress curves for plain but also reinforced concrete were compared with test results made on plain concrete.

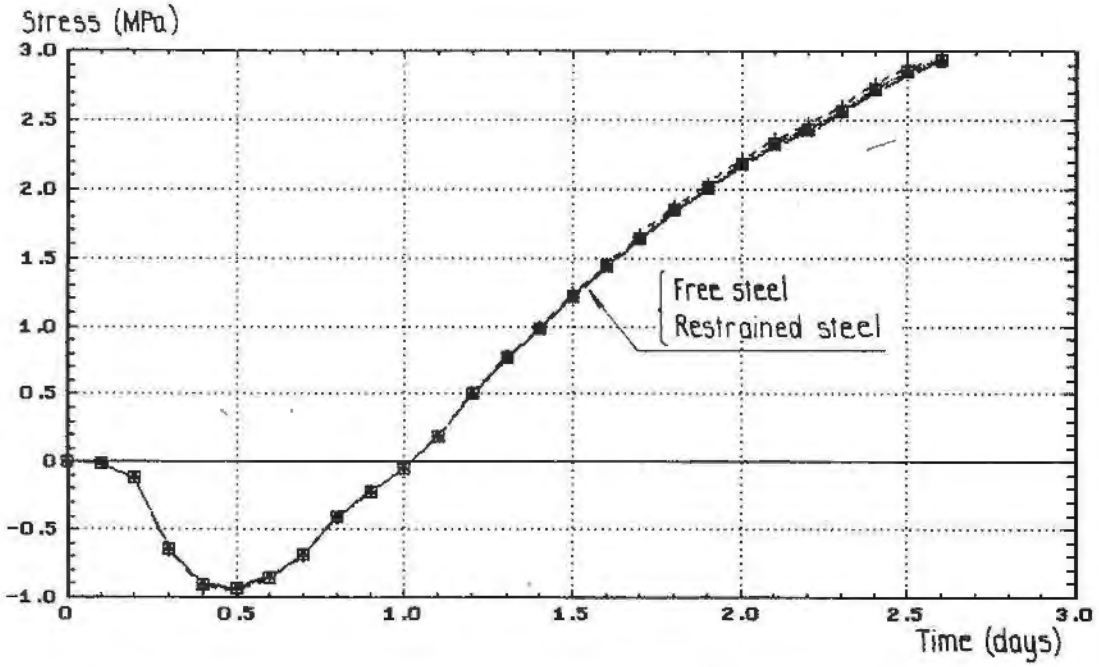

Fig.19. Stress in concrete S279 for different boundary conditions.

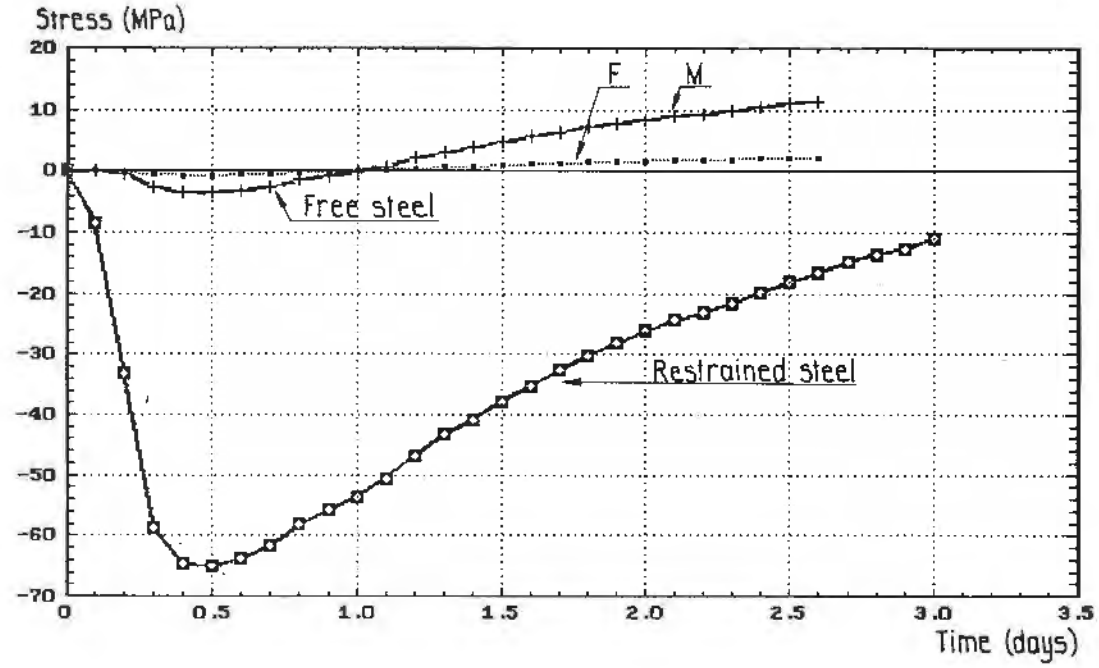

Fig.20. Stress in reinforcement for S279.

The presence of reinforcement does not improve the behaviour of the early age concrete prior to cracking for any of the two qualities. In view of its simplicity, the model gave a very good agreement with relaxation tests for plain concrete. It is quite obvious that a model on this level can be used to estimate thermal stresses with an accuracy which is sufficient for most practical purposes. Parametric investigations showed that temperature history, especially the maximum temperature rise, has a very significant influence on the risk of cracking. The rate of hydration or the concrete stiffness development with age is also very important for the development of thermal cracking. The magnitude of the thermal stresses is very sensitive to the timing between temperature rise and growth in stiffness. A cement which develops stiffness as early as possible and temperature increase as late as possible is very advantageous with regard to thermal cracking.

Compared to these effects creep and non-linear material behaviour, which often are elaborated in more advanced models, are much less significant. To obtain a good precision in the prediction it is very important to know the age dependence of the material stiffness.

The model can simulate the concrete behaviour correctly only until the stress reaches the tensile strength and therefore cannot describe the post-cracking behaviour. An obvious further development of the model is to introduce fracture mechanics, which would allow simulation of cracks in the concrete.

6. References

/1/ Springenschmid R. : Die Ermittlung der Spannungen infolge von Schwinden und Hydratationswärme in Beton. Beton und Stahlbetonbau, Vol 79, Heft 10, pp 263-269.

/2/ Breitenbücher R : Zwangspannungen und Riesbildungen infolge Hydratationswärme. Dissertation. Baustoffinstitut, Technische Universität, München 1989.

/3/ Emborg M. : Thermal stresses in concrete structures at early ages. Doctoral thesis 1989:73 D. Luleå University of Technology.

/4/ Hagman A. : Thermal stresses in concrete at early ages (in Swedish). Diploma work. TVBK-5050, March 1991, Dep. of Structural Engineering, Lund University.

/5/ Kasai Y.et.al.: Tensile properties of early age concrete (the plastic and elastic strain and the extensibility). Proceedings of the 1974 Symposia on Mechanical Behaviour of Materials. Kyoto, August the 21-24th, 1974, pp.433-441.

/6/ Dahlblom O., Peterson A. : CAMFEM - Computer aided modelling based on the finite element method. Report TVSM-3001, 1982, Lund Institute of Technology.

/7/ Ottosen N.S.,Petersson H. : Introduction to the finite element method. Report TVSM-3014, 1991, Lund University.